

EVALUATION OF WIND AND TURBULENT PARAMETERISATIONS FOR SHORT RANGE AIR POLLUTION MODELING

*D. Yordanov*¹, *M. Kolarova*², *U. Rizza*³, *C. Mangia*³, *T. Tirabassi*⁴, *D. Syrakov*²

¹ Geophysical Institute, Bulgarian Academy of Sciences, Acad. G. Bonchev str., bl. 3, Sofia 1113, Bulgaria

² National Institute of Meteorology and Hydrology, BAS, Tsarigradsko chausse Blvd. 66, Sofia 1784, Bulgaria, email: maria.kolarova@meteo.bg

³ Institute ISAC, CNR, Via Monteroni 4, Lecce, Italy, email: rizza@le.isac.cnr.it

⁴ Institute ISAC, CNR, Via P. Gobetti, 101, Bologna 40129, Italy, email: t.tirabassi@isac.cnr.it

Abstract. Most of the air quality dispersion models used for regulatory applications are based on K-diffusion formulations. In this paper, two turbulent parameterisations for dispersion models in the atmospheric boundary layer are evaluated with experimental data. The first scheme is based on a similarity approach and provides wind and eddy diffusivity profiles on the basis of a diagnostic PBL model. The second one provides an eddy diffusivity profile based on the Taylor statistical diffusion theory and on the spectral properties of turbulence. The two parameterisations have been included in a numerical grid model and tested with the Copenhagen data set. Results show that: i) the dispersion model with both turbulent schemes, produces a good fitting of the measured ground-level concentration data for all the experimental conditions considered; ii) there are no significant differences between the two schemes in the range of experimental data - the profiles are close to each other in the lower layers while they show larger differences in the layer above the surface layer. Therefore, both parameterisations give a realistic description of the dispersion processes in the lower PBL, and can be used for short range air pollution models and ground level concentrations.

Key words: turbulence parameterisations, planetary boundary layer, eddy diffusivities, air pollution modelling.

1. Introduction

The Eulerian approach is widely used in the field of air pollution studies to model the statistical properties of the concentrations of contaminants emitted in the Planetary

Boundary Layer (PBL). In this context, the diffusion equation that describes the cross-wind integrated concentrations arising from a continuous point source, where the along-wind diffusion is neglected, can be written as:

$$\frac{\partial \bar{c}}{\partial t} + \bar{u}(z) \bar{c} = -\frac{\partial \overline{w'c'}}{\partial z} + S, \quad (1)$$

where \bar{c} is the crosswind-integrated concentration, \bar{u} is the mean horizontal wind speed, $\overline{w'c'}$ is the vertical turbulent contaminant flux, and S is the sink/source term. One of the most widely used scheme for closing the eq. (1), is to relate the turbulent fluxes to the gradient of the mean concentration by mean of eddy diffusivity (K-theory):

$$\overline{w'c'} = -k_z \frac{\partial \bar{c}}{\partial z} \quad (2)$$

where k_z is the eddy diffusivity which must be evaluated using empirical data.

The simplicity of the K-theory has led to the widespread use of this theory as mathematical basis for simulating urban. But K-closure has its own limits: it works well when the dimension of dispersed material is much larger than the size of turbulent eddies involved in the diffusion process, i.e. for ground-level releases and for large travel times. Despite these well known limits, the K-closure is largely used in several atmospheric conditions because it describes the diffusive transport in an Eulerian framework where almost all measurements are Eulerian in character, it produces results that agree with experimental data as well as any more complex model, and it is not computationally expensive as higher order closures are.

The reliability of the k-approach strongly depends on the way the eddy diffusivity is determined on the basis of the turbulence structure of the PBL and on the model ability to reproduce experimental diffusion data. Keeping the K-theory limitations in mind many efforts have been made to develop turbulent parameterisations for practical applications in air pollution modelling which reveals the essential features of the turbulent diffusion, but which as far as possible preserves the simplicity and flexibility of the K-theory formulation. A variety of formulations for wind and eddy diffusivity exist (Yordanov et al., 1997; Yordanov et al., 1998; Ulke, 2000; Mangia et al., 2002; Djolov et al., 2004).

Aim of this paper is to evaluate two parameterisations for the velocity and eddy diffusivity profiles in PBL using a numerical grid model (Rizza et al. 2003) and to compare with Copenhagen dataset in order to discuss limits and possibilities of both parameterisations in view of their applications in air pollution studies.

The first model, which calculates the wind and eddy diffusivity profiles in the PBL under different stability conditions, is based on similarity theory. It is used in air pollution tasks accounting for two approaches – “top-down” and “bottom-up” as shown by Yordanov et al. (2004). In the “bottom-up” approach applied in this paper the PBL profiles are obtained applying YORDAN model (Yordanov et al., 2003) from the surface turbulent fluxes defined by the Monin-Obukhov length scale, L , and the friction velocity u_* , which are taken from the experimental data.

The second model is based on the Taylor's statistical theory and a model for Eulerian spectra (Olesen et al., 1984; Degrazia et al., 1992, Degrazia et al., 1997; Mangia et al., 2000). The main idea of the proposed spectral model relies on considering the turbulent spectra as a superposition of a buoyant produced part (with a convective peak wavelength) and a shear produced part (with a mechanical peak wavelength). By such a model, the plume spreading rate is directly connected with the spectral distribution of eddies in the PBL, that is with the energy containing eddies of the turbulence.

2. The PBL model YORDAN

The simple two-layer model (Yordanov et al., 1983) is used to produce the vertical profiles of the wind and the vertical turbulent exchange coefficient. The PBL model YORDAN was compared with a number of experimental data sets and demonstrates good coincidence as shown by Yordanov et al. (1998). The PBL model consists of a Surface Layer (SL) with height h_* and an Ekman layer above it.

In the SL, $z \leq h_*$, the wind profile is determined as:

$$\kappa \frac{u(z)}{u_*} = \begin{cases} \ln(z/z_0) + 10\zeta & \zeta \geq \zeta_0, \mu \geq 0 \\ \ln(z/z_0) & -0.07 \leq \zeta \leq \zeta_0, \mu < 0 \\ \ln(-0.07/\zeta_0) + 3[1 + (0.07/\zeta)^{1/3}] & \zeta \leq -0.07, \mu < 0 \end{cases} \quad (3)$$

where $\mu = \frac{\kappa u_*}{fL}$ is the internal stratification parameter, $\kappa = 0.4$ is the Von Karman constant, $\zeta = z/L$ is the non-dimensional height, $\zeta_0 = z_0/L$ is the non-dimensional roughness, and f is the Coriolis parameter ($f = 10^{-4} s^{-1}$).

For the non-dimensional SL height $h(\mu)$ the following relations are used:

$$h(\mu) = \begin{cases} 0.28/\mu, & \mu \geq 9.2 \\ 0.03, & -9.2 < \mu < 9.2 \\ 0.01|\mu|^{1/2}, & \mu \leq -9.2 \end{cases} \quad (4)$$

For the non-dimensional turbulent exchange coefficient K_m we have:

$$K_m = \begin{cases} Z/(1+10\mu Z), & Z_0 \leq Z \leq h, \mu \geq 0 \\ Z, & Z_0 \leq Z \leq (-0.07/\mu), -9.2 < \mu < 9.2. \\ (-0.07/\mu)^{-1/3} Z^{4/3}, & (-0.07/\mu) \leq Z \leq h, \mu \leq -9.2 \end{cases} \quad (5a)$$

For the dimensional turbulent exchange coefficient for momentum we have :

$$k_z = (\kappa^2 u_*^2 / f) K_m \quad (5b)$$

Here, we use the following relations: $h = h_* / H$ is the non-dimensional SL height, $H = \kappa u_* / f$ is the height scale, $Z = z / H$ is the non-dimensional height, and $Z_0 = z_0 / H$ is the non-dimensional roughness and for the dimensional SL height we obtain the relation: $h_* = h \kappa u_* / f$.

In the Ekman layer ($Z > h$), the turbulent exchange coefficient is assumed not to change with height and to be equal to K_{mh} , i.e. following (5) we obtain:

$$K_{mh} = \begin{cases} h / (1 + 10\mu h), & \mu \geq 0 \\ h, & -9.2 < \mu < 9.2 \\ (-0.07 / \mu)^{-1/3} h^{4/3}, & \mu \leq -9.2 \end{cases} \quad (6a)$$

The dimensional turbulent exchange coefficient for momentum is the obtained by:

$$k_z = k_{zh} = (\kappa^2 u_*^2 / f) K_{mh} \quad (6b)$$

The velocity components u and v at height z are calculated from the relations:

$$u = |v_g| \cos \alpha' + P \frac{u_*}{\kappa} \quad \text{and} \quad v = |v_g| \sin \alpha' + Q \frac{u_*}{\kappa}, \quad (7)$$

where α' is the cross-isobaric angle, u_g, v_g are the geostrophic wind velocities components and the non-dimensional velocity defects P and Q are given by the following expressions:

in SL:

$$P = \begin{cases} \ln(Z/h) + 10\mu(Z-h) - (2K_m)^{-1/2}, & Z_0 \leq Z \leq h, \quad \text{at } \mu \geq 0 \\ \ln(-\mu Z / 0.07) - 3[1 - (-0.07 h / \mu)^{1/3}] - (2K_m)^{-1/2}, & Z_0 \leq Z \leq (-0.07 / \mu), \\ -3[(-0.07 Z / \mu)^{1/3} - (-0.07 h / \mu)^{1/3}] - (2K_m)^{-1/2}, & (-0.07 / \mu) \leq Z < h, \quad \mu < 0 \end{cases} \quad (8)$$

and above SL:

$$P = -\exp(-\psi) [\cos \psi - \sin \psi] / (2K_{mh})^{1/2}, \quad \text{at } Z \geq h, \quad (9a)$$

and for the velocity defect in vertical direction we have:

$$Q = \begin{cases} (2K_m)^{-1/2}, & \text{at } Z \leq h \\ \exp(-\psi) (\cos \psi + \sin \psi) / (2K_{mh})^{1/2}, & \text{at } Z > h \end{cases} \quad (9b)$$

In Eq. (9a) and Eq. (9b) $\psi = (Z - h) / (2K_{mh})^{1/2}$, and the x-axis is directed along the surface wind.

Replacing the expressions from Eq. (8) and (9) in Eq. (7) we can find the velocity profiles given by the relation:

$$\bar{u}(z) = |u| = \sqrt{u^2 + v^2} \quad (10)$$

3. The spectral parameterization scheme

Following Batchelor (1953), Taylor (1921), and Pasquill and Smith (1983), under the hypothesis of homogeneous turbulence, the eddy diffusivities may be expressed as:

$$K_\alpha = \frac{d}{dt} \left(\frac{\sigma_\alpha^2}{2} \right) = \frac{\sigma_i^2 \beta_i}{2\pi} \int_0^\infty F_i^E(n) \frac{\sin(2\pi nt / \beta_i)}{n} dn \quad (11)$$

where $\alpha = (x, y, z)$ and $i = (u, v, w)$, $F_i^E(n)$ is the value of the Eulerian spectrum of energy normalized by the Eulerian velocity variance, and σ_i^2 corresponds to the Eulerian variance of the turbulent wind field.

Following (Wandel and Kofoed-Hansen, 1962) we can write that:

$$\beta_i = \left(\frac{\pi U^2}{16 \sigma_i^2} \right)^{1/2} \quad (12)$$

For large diffusion travel times ($t \rightarrow \infty$), the filter function in the integral of eq. (11) selects $F_i^E(n)$ at the origin of the frequency space, such that the rate of dispersion becomes independent of the travel time from the source and can be expressed as a function of local properties of turbulence as follows:

$$K_\alpha = \frac{\sigma_i^2 \beta_i F_i^E(0)}{4}, \quad (13)$$

where $F_i^E(0)$ is the value of the normalised Eulerian energy spectrum at $n = 0$.

In this way the eddy diffusivity is directly associated to the energy-containing eddies which are the most responsible of turbulent transport.

In order to utilize eq. (13) we have to find an analytical form for the dimensionless Eulerian spectrum. We assume here that the spectral distribution of turbulent kinetic energy is a superposition of buoyancy and shear components. Such a TKE model may be evaluated as a good approximation for a real PBL, where turbulent production is due to both mechanisms (Hojstrup, 1982; Moeng e Sullivan, 1994). In these conditions we may write for the Eulerian dimensional spectrum as:

$$S_i^E(n) = S_{ib}^E(n) + S_{is}^E(n), \quad (14)$$

where the subscripts b and s stand for *buoyancy* and *shear* respectively.

An analytical form for the dimensional spectra in convective turbulence has been found to be following (Degrazia et al., 1997):

$$S_{ib}^E(n) = \frac{0.98c_i(nz/\bar{u})}{n(f_{mi}^*)^{5/3} \left[1 + 1.5 \left((nz/\bar{u})/f_{mi}^* \right)^{5/3} \right]} \Psi_{eb}^{2/3} (z/z_i)^{2/3} w_*^2, \quad (15a)$$

while for the mechanical turbulence according (Degrazia and Moraes, 1992) we have:

$$S_{is}^E(n) = \frac{1.5c_i(nz/\bar{u})}{n(f_{mi}^*)^{5/3} \left[1 + 1.5 \left((nz/\bar{u})/f_{mi}^* \right)^{5/3} \right]} \Phi_{\varepsilon_s}^{2/3} u_*^2 \quad (15b)$$

where $\Phi_{\varepsilon_s} = \frac{\varepsilon_s K z}{u_*^3}$ and $\Psi_{eb} = \frac{\varepsilon_b h}{w_*^3}$ are the dimensional dissipation rate functions, and

ε_s and ε_b are the mechanical and convective rates of TKE dissipation, f_{mi}^* is the normalized frequency of the spectral peaks regardless of stratification and $nz/\bar{u} = f$ is the reduced frequency with \bar{u} the mean wind speed in the mixing layer. All the values of the constants are given in Appendix A.

The adimensional spectra $F_i^E(n)$ in eq. (13) is obtained by normalizing the dimensional spectra with the total variance:

$$\sigma_i^2 = \int_0^\infty S_i^E(n) dn, \quad (16)$$

that is:

$$F_i^E(n) = \frac{S_i^E}{\sigma_i^2} = \frac{S_{ib}^E(n) + S_{is}^E(n)}{\sigma_i^2} \quad (17)$$

The total wind velocity variance is obtained by the sum of mechanical and convective variances:

$$\sigma_i^2 = \int_0^\infty (S_{ib}^E(n) + S_{is}^E(n)) dn = \sigma_{ib}^2 + \sigma_{is}^2 \quad (18)$$

Making use of eqs. (13, 15a, 15b) and eq. (17) we can write:

$$K_\alpha = \frac{\beta_i}{4} (S_{ib}^E(0) + S_{is}^E(0)) \quad (19a)$$

which for the w-component becomes:

$$k_z = \frac{\beta_w}{4} \left(\frac{0.98c_w(z/\bar{u})}{(f_{mw}^*)^{5/3}} \Psi_{eb}^{2/3}(z/z_i)^{2/3} w_*^2 + \frac{1.5c_w(z/\bar{u})}{(f_{mw})^{5/3}} \Phi_{eb}^{2/3} u_*^2 \right) \quad (19b)$$

The wind speed profile used has been parameterised as follow:

For an unstable PBL ($L < 0$) the wind is given as:

$$\bar{u}(z) = \frac{u_*}{\kappa} \left[\ln(z/z_0) - \Psi_m(z/L) + \Psi_m(z_0/L) \right] \quad \text{at } z \leq z_b \quad (20a)$$

$$\bar{u}(z) = \bar{u}(z_b) \quad \text{at } z > z_b, \quad (20b)$$

where $z_b = \min[L, 0.1z_i]$ is the SL height, z_i is the height of the inversion layer, and

Ψ_m is a stability function given as: $\Psi_m = 2 \ln \left[\frac{1+A}{2} \right] + \ln \left[\frac{1+A^2}{2} \right] - 2 \tan^{-1}(A) + \frac{\pi}{2}$,

with $A = (1 - 16z/L)^{1/4}$.

For a stable PBL ($L > 0$) we use the relations:

$$\bar{u}(z) = \frac{u_*}{\kappa} \left[\ln(z/z_0) + \Psi_m(z/L) \right], \quad (21)$$

where the function Ψ_m is given by the expression: $\Psi_m \left(\frac{z}{L} \right) = 4.7 \left(\frac{z}{L} \right)$

5. The numerical grid model

In order to test the eddy diffusivity parameterizations proposed, we used the numerical grid model named APUGRID (Rizza et al. 2003). The model was developed using the numerical technique based on Fractional Step/Locally One Dimensional method (Yanenko, 1971; Mc Rae et al., 1982; Marcucci, 1984). It consists in splitting eq. (1) into a set of time dependent equations, each one Locally One Dimensional (LOD):

$$\frac{\partial \bar{c}}{\partial t} = \sum_{i=1}^3 \Lambda_i, \quad (22)$$

where

$$\Lambda_i = A_i + D_i \equiv -\bar{u}_i \frac{\partial}{\partial x_i} + \frac{1}{S_c} \frac{\partial}{\partial x_i} \left(K_c \frac{\partial}{\partial x_i} \right). \quad (23)$$

Using Crank-Nicholson time integration we have:

$$\bar{c}^{-n+1} = \prod_{j=1}^3 \left[I - \frac{\Delta t}{2} \Lambda_j \right]^{-1} \left[I + \frac{\Delta t}{2} \Lambda_j \right] \bar{c}^{-n} = \prod_{j=1}^3 T_j^n \bar{c}^{-n} \quad (24)$$

where I is the unity matrix.

To obtain second order accuracy, it is necessary to reverse the order of the operators each alternate step to cancel the two non-commuting terms. We have to replace the scheme given by eq. (24) with the following double-sequence equations:

$$\bar{c}^{-n} = \prod_{j=1}^3 T_j^n \bar{c}^{-n-1} \quad (25a)$$

$$\bar{c}^{-n+1} = \prod_{j=3}^1 T_j^n \bar{c}^{-n} \quad (25b)$$

In order to develop a scheme that preserves peaks, retain positive quantities, and does not severely diffuse sharp gradients, after each advective step a filtering procedure is necessary for damping out the small scale perturbations before they can corrupt the basic solution. So, the effective system utilized is the following:

$$\bar{c}^{-n} = \prod_{i=1}^3 [A_i F D_i] \bar{c}^{-n-1} \quad (26)$$

$$\bar{c}^{-n+1} = \prod_{i=1}^3 [D_i A_i F] \bar{c}^{-n} \quad (27)$$

where the operator F represents the filter operation.

The advection terms are calculated with a semi-lagrangian cubic spline technique following (Pielke, 1984), while diffusive terms are calculated with Crank-Nicholson implicit scheme. To avoid unwanted numerical noises produced by the advection numerical scheme a non-linear filter (Forester, 1979) was used. The model has been validated using wind/turbulence data generated with a Large Eddy Simulation (Rizza et al., 2003).

6. PBL models evaluation

6.1 Experimental data

The two PBL models described above have been included in the numerical model APUGRID and evaluated with the Copenhagen data set (Gryning and Lyck, 1984; Gryning and Lyck, 2002). The Copenhagen data set is composed of tracer SF_6 data from dispersion experiments carried out in northern Copenhagen. The tracer was released without buoyancy from a tower at a height of 115 m and was collected at ground-level positions in up to three

crosswind arcs of tracer sampling units. The sampling units were positioned 2-6 km far from the point of release. Tracer releases typically started up 1 hour before the tracer sampling and stopped at the end of the sampling period. The site was mainly residential with a roughness length of 0.6 m. The meteorological measurements performed during the experiments included standard measurements along the tower of tracer release. The meteorological conditions during the dispersion experiments considered ranged from moderately unstable to convective. Table 1 summarises the meteorological conditions during the Copenhagen experiment used as input data for the PBL models simulations.

Table 1. Summary of the meteorological input data from the Copenhagen experiment used in the simulations.

Experiment No - day	U_s m/s	u_* m/s	L m	w_* m/s	z_i m	$\mu_c = z_i/L$
1 - Sept. 20	3.4	0.36	-37	1.7	1980	-53.5
2 - Sept. 26	10.6	0.73	-292	1.8	1920	-6.6
3 - Oct. 19	5.0	0.38	-71	1.3	1120	-15.8
4 - Nov. 3	4.6	0.38	-133	0.7	390	-2.9
5 - Nov. 9	6.7	0.45	-444	0.7	820	-1.8
6 - April 30	13.2	1.05	-432	2.0	1300	-3.0
7 - June 27	7.6	0.64	-104	2.2	1850	-17.8
8 - July 6	9.4	0.69	-56	2.2	810	-14.5
9 - July 19	10.5	0.75	-289	1.9	2090	-7.2

U_s is the wind speed at the source height, L is Monin-Obukhov length scale, u_* - friction velocity w_* - the convective velocity scale, z_i is the height of the inversion layer and μ_c is the internal stratification parameter for convective condition.

6.2 Results and discussion

To test the PBL parameterisations described before we simulate the different Copenhagen experiments calculating the turbulent profiles taking as input data the parameters given in Table 1. Applying the APUGRID dispersion model with both parameterisations we calculate the crosswind integrated concentrations at the ground and compare with the experimental data applying a well-known statistical procedure for the indices.

Figure 1 shows the comparison between wind velocity profiles $\bar{u}(z)$ obtained with the two PBL models described before plotted as function of normalized to z_i height and simulating the different experimental cases from Table 1. Model I refers to the PBL model YORDAN, where the mean wind is calculated according eqs. (3) (7) and (10), while Model II refers to eqs. (20a) and (20b). The wind profiles produced by the two models are close to

each other at lower heights (approximately below 100 m) and differs at greater heights, where Model I produces higher velocities, while Model II assumes constant values. The comparison with measured data at different heights is plotted by dots. We find the comparison with the experimental data satisfactory for both PBL models.

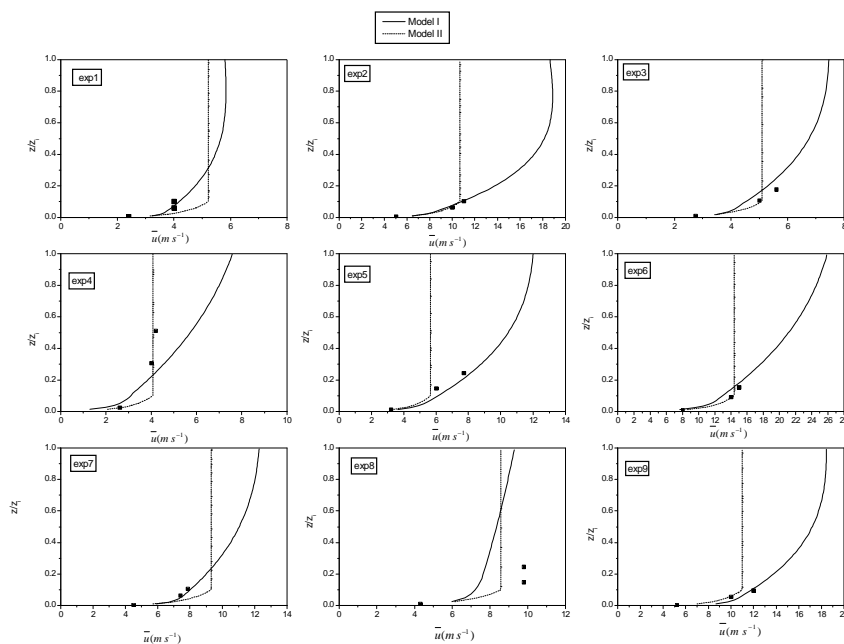


Fig. 1 Comparison between wind velocity profiles given by Model I (solid line) and Model II (dotted line) for the different Copenhagen experiments (No1-No9). Model I is given by eqs. (3) (7) and (10), while Model II is given by eqs. (20a) and (20b). The measured data are plotted with squares.

In the range of the heights of measured data both models simulate the experimental wind velocity $\bar{u}(z)$ quite well as can be seen from Figure 2, where a scatter diagram for the measured and predicted velocities below 200m is shown. Here again Model I is given by eqs. (3) (7) and (10), while Model II is given by eqs. (20a) and (20b).

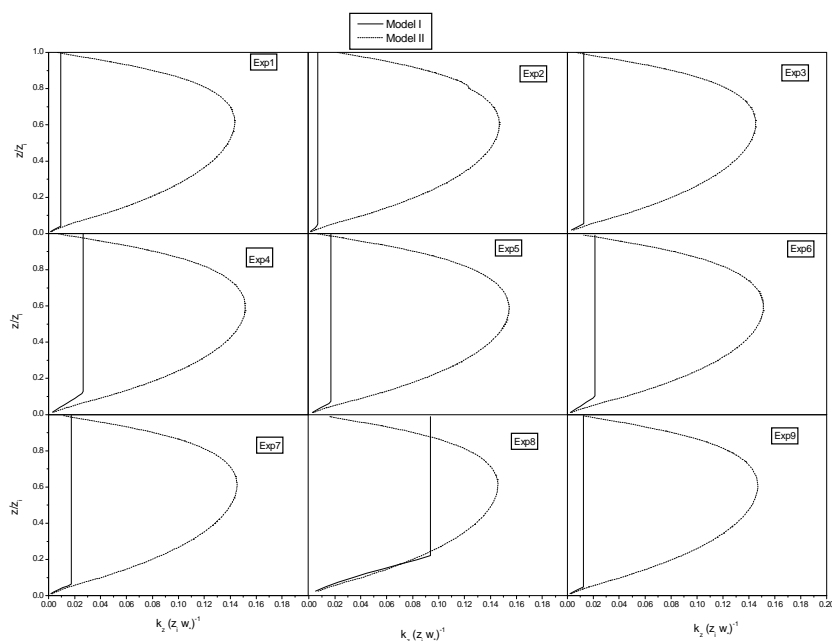


Fig. 3. Comparison between eddy diffusivity profiles $k_z(z)$ obtained with Model I according to eqs. (5) and (6) and Model II given by eq. (19) calculated for the different Copenhagen experiments.

In Figure 3 a comparison between the eddy diffusivity profiles $k_z(z)$ obtained with the two models is presented for the same cases as those shown in figure 1. Model I refers to YORDAN PBL model with k -profiles given by eqs. (5) and (6), while Model II is given by eq. (19). Figure 3 shows that eddy diffusivity profiles $k_z(z)$ are closer at lower z (around 100m) and in the surface layer, while above it Model II gives much bigger values for $k_z(z)$ in comparison to those obtained by the Model I which assumes constant values in the Ekman Layer.

Figure 4 shows a scatter diagram of the observed and predicted ground-level crosswind integrated concentrations (normalized with the emission source rate) using APUGRID model with the different wind and eddy diffusivity profiles. Model I is obtained with YORDAN parameterisation applying eqs. (3) and (7 - 10) for the wind speed profiles, and eqs. (5 - 6) for eddy diffusivity profiles. Model II is realized by using spectral parameterization scheme for $k_z(z)$ according to eq. (19) and for the wind speed profile according to eqs. (20a) and (20b). The points placed between the dashed lines are in a factor of two.

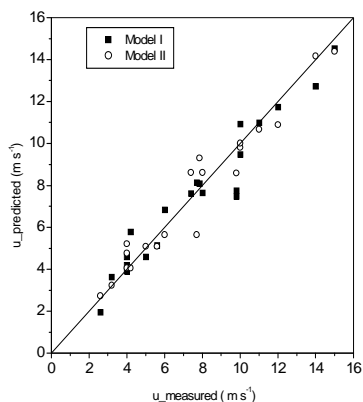


Fig. 2. Comparison between the predicted and measured wind velocities at different heights below 200m for all Copenhagen experiments.

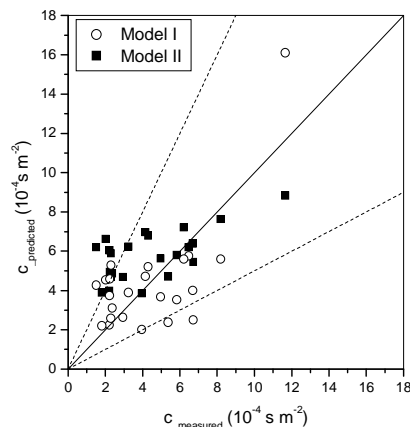


Fig. 4. Comparison between observed and predicted cross-wind integrated ground level concentrations normalized with the emission source rate.

In Figure 5 the observed and computed by the two models (Model I and Model II) ground level concentrations (c) as a function of the source distance are compared for each Copenhagen experiment.

From Figure 5 it can be seen that, Model I gives lower surface cross-wind concentrations in comparison to Model II (except for the experiment 4). These differences can be explained with the behavior of the wind and eddy diffusivity profiles presented in figures 1 and 2. Higher $k_z(z)$ given by Model II at higher z can be the explanation for these differences. The opposite behavior shown for the experiment No 4, where Model I gives higher concentrations than Model II can be related to the low value of the measured mixing layer ($z_i = 390\text{m}$) and to the corresponding stratification which was close to adiabatic one with relatively low wind velocities (4.6 m/s) and low friction velocity ($u_* = 0.38\text{m/s}$).

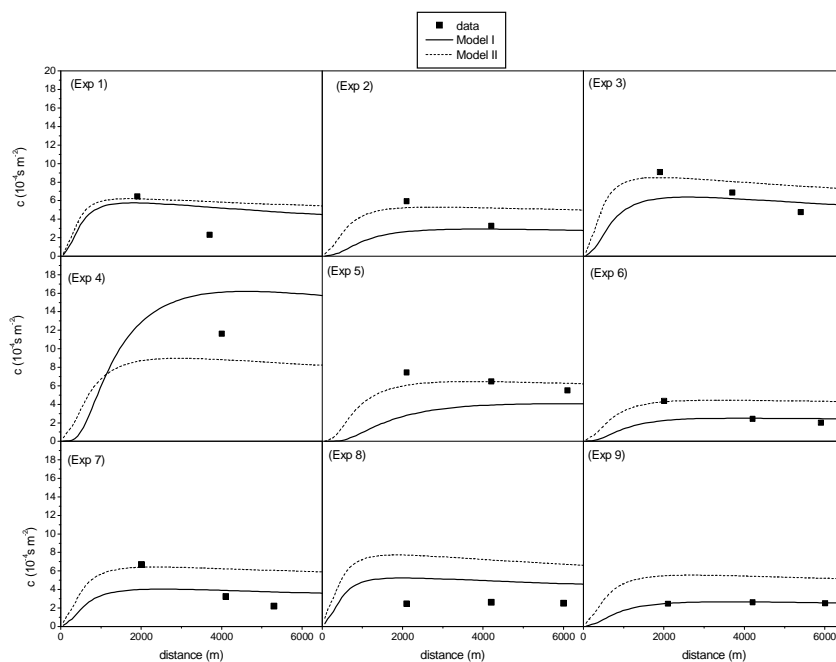


Fig. 5. Comparison of the ground level observed data with the cross-wind integrated concentrations predicted by APUGRID dispersion model as function of the distance from the source, applied with the different PBL parameterisations. Model I and Model II are the same as in Fig. 4. Dots are the measured data.

An evaluation of the performances given by the two models, using BOOTSTRAP procedure, described by Hanna (1989) is presented in Table 2. Statistical indices defined in the following way were utilized:

$$\text{NMSE (normalized mean square)} = \overline{(C_o - C_p)^2} / \overline{C_o C_p};$$

$$\text{COR (correlation)} = \overline{(C_o - \overline{C_o})(C_p - \overline{C_p})} / \sigma_o \sigma_p;$$

FA2 = fraction of C_o values within a factor two of corresponding C_p values;

$$\text{FB (fractional bias)} = (\overline{C_o} - \overline{C_p}) / (0.5(\overline{C_o} + \overline{C_p}));$$

$$\text{FS (fractional standard deviations)} = (\sigma_o - \sigma_p) / 0.5(\sigma_o + \sigma_p),$$

where the subscripts o and p refer respectively to observed and predicted quantities, and the over-bar indicates an average.

Table 2. Statistical indices evaluating the performances of the two model considered.

Models	NMSE	COR	FA2	FB	FS
Model I	0.24	0.67	0.74	-0.004	-0.11
Model II	0.23	0.64	0.65	-0.29	0.67

Results and relative statistics highlight a satisfactory performance of the two models proposed for all the experiments considered. There is a good correlation between predictions and experimental data in particular the highest concentration values (the most important for regulatory purposes) are within a factor of two of data. Model II seems to reproduce better the highest values close to the source while tends to over predict data far-away of the source emission which are fitted better by the Model I. Anyway, all the values for the numerical indices are within ranges that are characteristic of those found for other state-of-the-art models applied to other field datasets (Hanna, 1989).

7. Conclusions

Two different wind and eddy diffusivity schemes have been evaluated in this paper using a numerical grid model. The first one is based on a similarity approach and derives wind and eddy diffusivity profiles on the basis of a unique PBL model (YORDAN) resulting more physically consistent. The other approach provides an eddy-diffusivity profile based on the Taylor statistical diffusion theory and on the spectral properties of turbulence. The assumption of continuous turbulence spectrum and variances, allows the parameterisations to be continuous at all elevations, and in stability conditions ranging from convective to neutral, and from neutral to stable so that the simulation of a full diurnal cycle is possible.

Both schemes have been included in a grid numeric model and evaluated in several turbulent regimes using the Copenhagen data set where the source emission is at 115m.

Analysis of the results obtained and the application of well-known statistical indices show that both schemes considered produce a good fit for the experimental meteorological and ground level concentration data. There are not significant differences between the two schemes in the range of experimental data. The difference between the two models above the surface layer does not provide great differences in the ground level concentration pattern.

Results showed in the present paper confirm the applicability of the both PBL parameterisations for short-range air pollution modelling.

Acknowledgements. The authors thank to S.-E. Gryning for the supplied revised results from the Copenhagen experiment. This paper was done under the bilateral collaboration between Italian CNR and Bulgarian Academy of Sciences (BAS).

Appendix A

The values of the constants used in &3 are chosen following Table I (Olesen et al., 1984):

$$c_u = 0.3, \quad c_v = c_w = 0.4, \quad \text{and}$$

$$(f_m)_u = 0.045, \quad (f_m)_v = 0.16, \quad (f_m)_w = 0.35.$$

The stability function q_i is given by the expression:

$$q_i = \frac{(f_m^*)_i}{(f_m)_i} = \frac{z}{(f_m)_i (\lambda_m^*)_i},$$

where $(\lambda_m^*)_i$ are the spectral peak depending on height and stability given as:

$$(\lambda_m^*)_u = 1.5z_i \quad 0.01z_i \leq z \leq z_i, \quad \text{and} \quad (\lambda_m^*)_v = 1.5z_i \quad 0.01z_i \leq z \leq z_i, \quad \text{and}$$

$$(\lambda_m^*)_w = \begin{cases} z(0.55 - 0.38|z/L|)^{-1} & 0 \leq z \leq |L| \\ 5.9z & |L| \leq z \leq 0.1z_i \\ 1.8z_i(1 - e^{-4z/z_i} - 0.0003e^{8z/z_i}) & 0.1z_i \leq z \leq z_i \end{cases}.$$

The buoyancy/shear ensemble average rate of TKE dissipation are from Hojstrup (1982):

$$\varepsilon_b = (0.75)^{3/2} \frac{W_*^3}{z_i}, \quad \text{and} \quad \varepsilon_s = \frac{u_*^3}{\kappa z} \left(1 - \frac{z}{z_i}\right)^3.$$

References

- Batchelor, G.K. 1953. *The Theory of Homogeneous Turbulence*, 197pp., Cambridge University Press.
- Degrazia, G.A., and O.L.L.Moraes, 1992. A model for eddy diffusivity in a stable boundary layer, *Boundary Layer Meteorology*, **58**, 205-214.
- Degrazia, G.A., U.Rizza, C.Mangia, and T.Tirabassi, 1997. Validation of a new turbulent parameterisation for dispersion models in a convective boundary layer, *Boundary Layer Meteorology*, **85**, 243-254.
- Djolov, G.D., D.L.Yordanov, and D.E.Syrakov, 2004. Baroclinic PBL model for neutral and stable stratification conditions, *Boundary Layer Meteorology*, **111**, 467-490.
- Forester C.K., 1979. *J.Comp.Phys.*, **23**, 1.
- Gryning, S.E. and E.Lyck, 1984. Atmospheric dispersion from elevated sources in an urban area: Comparison between tracer experiments and model calculations, *J. Climate Appl. Meteor.*, **23**, 651-660.

- Gryning, S.E., A.A.M.Holtslag, J.S.Irwin and B.Siversten, 1987. Applied dispersion modelling based on meteorological scaling parameters, *Atmos. Environ.*, **21**, 79-89.
- Gryning, S.E. and E.Lyck, 2002. RISO-R-1054(rev.1) (En). *The Copenhagen Tracer Experiment: Reporting of measurements*, RISOE National Laboratory, Roskilde.
- Hanna, S.R., 1989. Confidence limits for air quality models, as estimated by bootstrap and jackknife resampling methods, *Atmospheric Environment*, **23**, 1385-1395.
- Højstrup, J., 1982. Velocity spectra in the unstable boundary layer, *J. Atmos.Sci.*, **39**, 2239-2248.
- Mangia C., G.A.Degrazia, and U.Rizza, 2000. An integral formulation for the dispersion parameters in a shear/buoyancy driven planetary boundary layer for use in a Gaussian model for tall stacks, *Journal of Applied Meteorology*, **39**, 1913-1922.
- Mangia, C., D.M.Moreira, I.Schipa, G.A.Degrazia, T.Tirabassi, and U.Rizza, 2002. Evaluation of a new eddy diffusivity parameterisation from turbulent Eulerian spectra in different stability conditions, *Atmos. Environ.*, **36**, 67-76.
- Marcuk, N.N., 1984. in *Metodi del Calcolo Numerico*, edited by Editori Riuniti, pp. 245-289, Roma.
- Mc Rae, G.J., W.R.Goodin, and J.H.Seinfeld, 1982, *J.Comp.Phys.*, **45**, 1.
- Moeng, C.H. and P.P.Sullivan, 1994. A comparison of shear-and buoyancy- driven planetary boundary layer flows, *J. Atmos. Sci.*, **51**, 999-1022.
- Olesen, H.R., S.E.Larsen, and J.Højstrup, 1984. Modelling velocity spectra in the lower part of the planetary boundary layer, *Bound. Layer Meteor.*, **29**, 285-312.
- Pasquill F., and F.B.Smith, 1983. Atmospheric diffusion. Ellis Horwood Ltd., 437 pp.
- Rizza U., G.Gioia, C.Mangia, and G.R.Marra, 2003. Development of a grid dispersion model in a large-eddy-simulation-generated PBL, *Il Nuovo Cimento*, **26C**, 3, 297-309.
- Taylor, G.I., 1921. Diffusion by continuous movement, *Proc. Lond. Math. Soc.*, **2**, 196-211.
- Ulke, A.G., 2000. New turbulent parameterisation for a dispersion model in the atmospheric boundary layer, *Atmospheric Environment*, **34**, 1029-1042.
- Yanenko, N.N., 1971. in *The Method of Fractional Steps*, edited by Springer-Verlag, pp.27-33, Berlin, New York.
- Yordanov, D., D.Syrakov, and G.Djolov, 1983. A Barotropic Planetary Boundary Layer, *Boundary Layer Meteorology*, **25**, 1-13.
- Yordanov D., D.Syrakov and M.Kolarova, 1997. On the Parameterization of the Planetary Boundary Layer of the Atmosphere, The Determination of the Mixing Height -Current Progress and Problems. EURASAP Workshop Proc., 1-3 Oct. 1997.
- Yordanov, D., D.Syrakov, , G.Djolov, 1998. Baroclinic PBL model: neutral and stable stratification condition, *Bulg. Geophys. J.*, **14**, No.1-2, 5-25.
- Yordanov, D.L., D.E.Syrakov, and M. P.Kolarova, 2003. Parameterization of PBL from the surface wind and stability class data, *Proc. of NATO ARW on Air Pollution Processes in Regional Scale*, Halkidiki, Greece, 13-15 June 2002, NATO Science Series, D.Melas and D.Syrakov (eds.), Kluwer Acad. Publ., Netherlands, Vol. 30, 347-364.
- Yordanov, D., M.Kolarova, and D.Syrakov, 2004. The ABL models YORDAN and YORCON—top-down and bottom-up approach for air pollution applications, *Proc. of NATO ARW "Advances in Air Pollution Modeling for Environmental Security"*, 8–12 May 2004, Borovetz, Bulgaria.
- Wandel, C.F., O.Kofoed-Hansen, 1962. On the Eulerian-Lagrangian Transform in the Statistical Theory of Turbulence, *Journal of Geophysical Research*, **67**, 3089-3093.

Параметризация на профилите на вятъра и коефициента на турбулентен обмен за моделиране на замърсяването на въздуха на близки разстояния

Д. Йорданов, М. Коларова, У. Рица, К. Манджа, Т. Тирабаси и Д. Сираков

Резюме. Голяма част от дисперсионните модели за качество на въздуха прилагани за решаване на регулаторни задачи използват К теорията. Параметризацията на профилите на вятъра и коефициента на турбулентен обмен съгласно най-новите разбирания за процесите в Атмосферния Граничен Слои (АГС) е от съществено значение при реализирането на този подход.

В настоящата статия се тестват две различни параметризационни схеми за профилите на вятъра и коефициента на турбулентен обмен в АГС чрез сравнение с експериментални данни. Първата е развита в българския диагностичен модел на Планетарния Граничен Слои (ПГС) YORDAN, който изчислява профилите на вятъра и коефициента на турбулентност на базата на теория на подобие на ПГС. Втората е включена в дифузионния модел APUGRID и изчислява коефициента на турбулентен обмен на базата на статистическата дифузионна теория на Тейлор и спектралната теория на турбулентността. Профилът на вятъра се параметризира съгласно Бусингер до височината на Приземния Слои (ПС), а след това е постоянен. Числения дисперсионен модел APUGRID е приложен за изчисляване на приземните концентрации при симулиране на експерименталните данни Копенхаген последователно с двете параметризационни схеми като са направени сравнения между реализациите. Получените резултати показват че: дисперсионният модел APUGRID приложен и с двете параметризации дава добро съвпадение с експерименталните данни за приземната концентрация от източник с височина 115м при различни стратификации на атмосферата; за профилите се показва добро съвпадение с експерименталните данни в ПС и различия над него. Това предполага, че дори при използване на различни параметризационни хипотези при реализиране на подходите, сравняваните параметризационни схеми описват реалистично турбулентните процеси в АПС и могат да се прилагат в задачите за моделиране на замърсяването на близки разстояния при изчисляване на приземните концентрации.